# Techniques of Field Survey

# 26

Frank Prendergast

## Contents



**Abstract**

Within the last decade in particular, geo-spatial measurement technologies have undergone significant advancement in terms of automation, processing, and levels of accuracy. These developments hold many advantages for archaeoastronomers engaged in the collection and analysis of field survey data. This chapter examines azimuth and location measuring techniques and assesses how some of the recent developments can assist those engaged in such fieldwork.

F. Prendergast
Spatial Information Sciences, College of Engineering and Built Environment, Dublin Institute of Technology, Dublin, Ireland
e-mail: frank.prendergast@dit.ie

C.L.N. Ruggles (ed.), *Handbook of Archaeoastronomy and Ethnoastronomy*,
DOI 10.1007/978-1-4614-6141-8_31,

## Introduction

Field surveys of prehistoric/historic sites and monuments are generally undertaken by archaeoastronomers to enable specific research questions to be addressed within culturally relevant frameworks and agendas. Investigations may, for example, be commissioned by an excavation director where the spatial setting or design of a discovered structure could suggest a function that cannot be explained by the material finds or other archaeological evidence alone (e.g., Prendergast 2012; O' Connell 2013). In all such cases, the spatial data element must first be recorded and processed to appropriate levels of quality.

Archaeoastronomers invariably come from diverse academic or professional backgrounds outside of (though not exclusively) archaeology. These include astronomy, surveying, engineering, mathematical sciences, science history, and computer science. The acquisition of spatial data, and its subsequent evaluation, can present many challenges. For some, the necessary field or analytical proficiencies may be established, but for most, a degree of specialized training or learning is required to redress a particular skill deficiency. This chapter will focus on field-surveying techniques and computational methods as commonly used during the initial stages of a site survey.

Pioneers of archaeoastronomy used nothing more than a theodolite, chain and compass in the field, and logarithmic tables or analogue calculators for data reduction (e.g., Somerville 1923; Thom 1967). Nonetheless, they achieved high-quality results and their legacies remain valid to this day – at least in terms of accuracy (as distinct from their interpretative outcomes in some cases). Moreover, certain aspects of computational theory and theodolite usage have not significantly changed either since those early surveys. Now, however, the digital revolution in measurement and positioning technologies, terrain modeling methods, mapping products, and landscape analysis software, all demand high levels of technical expertise in order to leverage their full potential. Many of the modern techniques can be complex, and any detailed description of their use is beyond the scope of this chapter. A comprehensive treatment of best surveying practice, and of horizon profile survey and data reduction techniques, has been published by Ruggles (1999, pp 164–171). Additionally, the orientation of visibility measurements has been described by Fraser (1988), and these need not be reconsidered in this chapter. Instead, and particularly for the benefit of those new to this field of study, more recent advances in surveying procedures, and updates to established methodologies where this is appropriate, are described here. Additional information drawn from case studies undertaken by the writer is also given elsewhere in this volume (see ▶ Chap. 107, "Irish Neolithic Tombs in Their Landscape"; ▶ Chap. 108, "Boyne Valley Tombs").

## Axis Before Azimuth

At the outset, attention is drawn to nomenclature and the terms "orientate/orientation" and "align/alignment". Here, orientation is taken to mean the measured direction of a structure's façade or axis with respect to the local meridian (azimuth), while the use of "aligned" is reserved for cases where human intentionality in a monument's axial direction toward a target is argued. The noun "alignment", however, can be archaeologically defined as meaning three or more related structures placed in a line. Where these conventions have not been rigorously followed in the literature and "orientation" loosely interchanged with "alignment", etc., Darvill (2002, p 301) correctly argues "...this is careless usage. All objects and structures will have an orientation whether or not anything is aligned on them".

The majority of archaeoastronomical surveys are undertaken to initially determine, inter alia, the orientation of a site, monument, or tomb. When combined with location (latitude) and profiles of the local horizon (azimuth and altitude), these data computationally yield astronomical declinations of the indicated positions of prominent celestial bodies of interest – either on the local horizon (rise/set), or of non-horizon events such as a transit phenomenon (see ▶ Chap. 30, "Basic Concepts of Positional Astronomy"; Kelley and Milone 2005, pp 9–47). Where combined with the date/period of construction (if known), declination is then commonly used to interpret any potential calendrical link or suspected ritual function in a cultural context.

A monument's axis is rightly regarded as the most enduring evidence of ancient architectural principles. Often, it functioned as a ceremonial entrance and pathway, and symbolically incorporated formality and power, especially if aligned on a prominent astronomical event or target. It is emphasized here that if deliberate alignment in the past toward any type of target was ever intended (it may not have been), an astronomical explanation is only one of a wide range of possible alternatives. These include an association with ritual topographies, local settlements, burial sites, or resources (see ▶ Chap. 25, "Best Practice for Evaluating the Astronomical Significance of Archaeological Sites").

## Structural Axis Definition

The morphological irregularity encountered in entrance passages can often defy any precise attempt to determine their mean axial line. In such cases, the careful positioning of the observer equipped with a handheld compass, theodolite, or gyro station (see section "Gyro Station Techniques") at one end of the axis line is all that may be required. Provided due care is taken to visually determine the best-fit line through the stones of the passage and entrance, the measured/derived azimuth (see below and section "Astronomical Azimuth Techniques and Instrumentation") of this line should adequately reflect the axial orientation of that structural element. Subsequently, the calculation of indicated astronomical declination may provide evidence of design or other intent.

In Fig. 26.1, for example, the unroofed/uncovered Neolithic court tomb at Creevykeel, Co. Sligo is shown. Here, the observer was positioned at P and was equipped with a handheld compass and inclinometer (see Fig. 26.2).

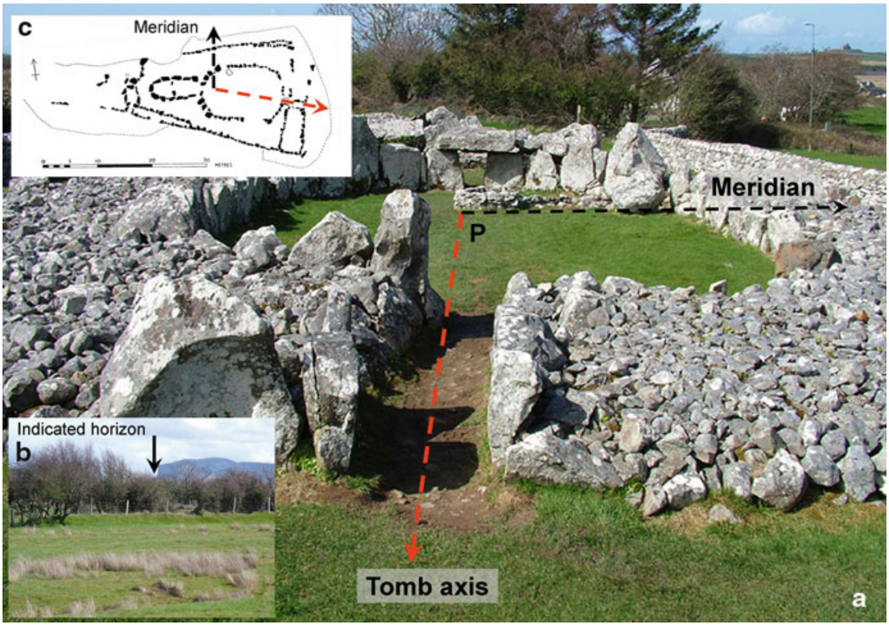


**Fig. 26.1** Creevykeel court tomb, Co. Sligo, Ireland. (**a**) The axial in-view of the tomb looking west. (**b**) The horizon to the east as indicated by the out-view through the passage. (**c**) A site plan with additions by the writer (source: de Valera 1960 Plate 1). The observed magnetic bearing of the axis (106°) was corrected for magnetic declination (–6° 17′). The axial azimuth (99° 43′), site latitude (+54° 26′ 19″), and horizon altitude (+1° 30′) yielded an astronomical declination (solar) of –4° 42′. Astronomical declination (solar and geocentric lunar) can also be determined by using Clive Ruggles' online calculator GETDEC (http://www.cliveruggles.net/)

These instruments were used to measure the magnetic bearing (clockwise direction with respect to local magnetic north) of the tomb axis and the altitude (angular distance above or below the horizon) of points on the distant skyline indicated by the axis, with an accuracy of about half a degree.

The magnetic declination at Creevykeel (angular deviation between magnetic and true north) was calculated using an algorithm obtained from the Irish Meteorological Service and by using the online NOAA magnetic field calculator (http://www.ngdc.noaa.gov/geomag-web/#declination). Both methods determined the declination component of the local magnetic field. The other components (inclination and total force) are not relevant here. Figure 26.2 illustrates the tools used in this type of survey.

It is evident from this survey that the orientation of the tomb suggests neither an interest in the horizon position of the rising sun at the solstices (winter or summer) or at the equinoxes (vernal/autumnal). This leaves open the possibility of a range of alternative interpretations including a random hypothesis (see ▶ Chap. 27, "Analyzing Orientations"; ▶ Chap. 33, "Lunar Alignments - Identification and Analysis"; ▶ Chap. 35, "Stellar Alignments - Identification and Analysis").

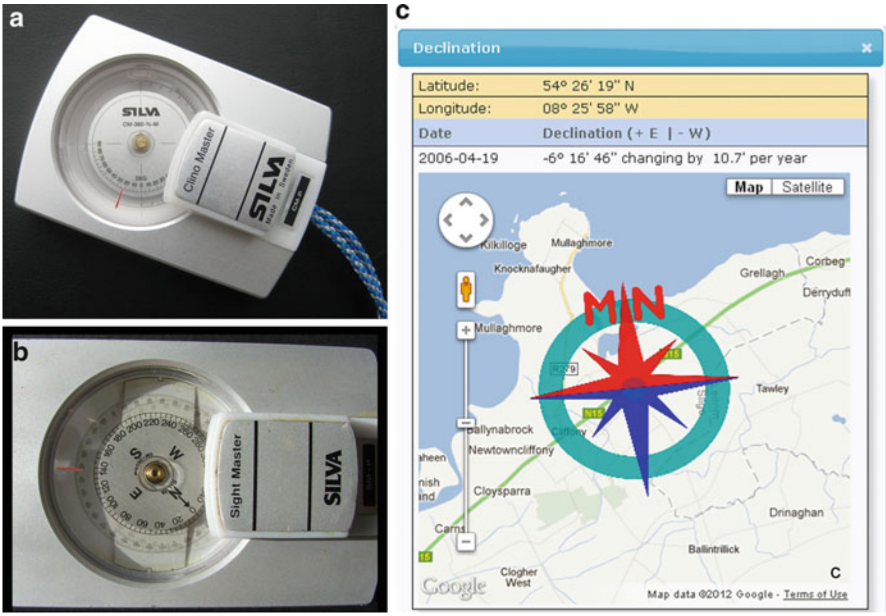


**Fig. 26.2** Tools for preliminary surveys of orientation and horizon altitude. (**a**) The Silva inclinometer (Clino Master) was used to measure local horizon altitudes to c. $\pm 0^\circ.5$. For an alternative method that utilizes digital elevation models to deduce horizon altitudes, see Patat (2011). (**b**) The Silva compass (Sight Master) was used to measure magnetic bearings to c. $\pm 0^\circ.5$. (**c**) A screen shot of the NOAA magnetic declination calculation for Creevykeel court tomb (courtesy of NOAA). Local values of declination for date and place can also be deduced from national maps. If an astronomical azimuth has been observed locally, the difference between azimuth and the magnetic bearing will also determine the magnetic declination at that place and calibrates the compass

For greater accuracy, the orientation of a line/axis can be numerically determined provided that the planimetric or grid coordinates of the defining points of interest have been measured in the national map projection system (see section "Geodetic Techniques for Azimuth Determination and Location"). This method can also to be applied to deduce the orientation of a building façade, regardless of its size. In Fig. 26.3, for example, the reconstructed architectural elements of a recently discovered Iron Age post enclosure at Lismullin, Co. Meath are shown. The national grid coordinates of all recovered postholes (only the buried sockets survived) were accurately recorded by archaeologists during the excavation by using a geo-referenced total station. This allowed linear regression analysis of the avenue data by the writer to calculate the mean axial orientation and goodness-of-fit of the avenue sides to the best-fit line.

In that analysis, the equation of each best-fit line through the postholes forming the north and south sides of the avenue takes the form

$$y = mx + c \tag{26.1}$$

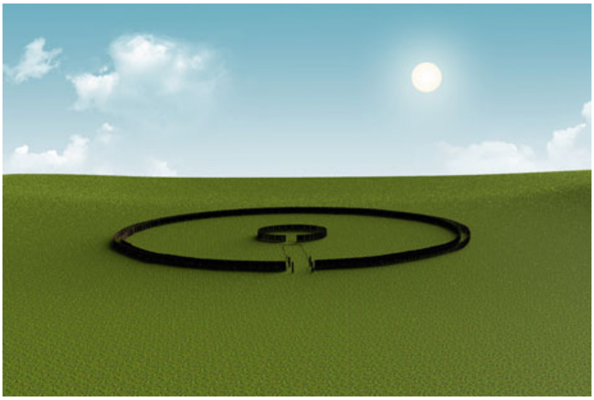

**Fig. 26.3** Iron Age post enclosure, Lismullin, Co. Meath. The structure consisted of three concentric rings formed of upright timber posts, and a 4 m wide easterly facing avenue. The avenue leads from the emphasized four-post entrance structure to a transverse depositional pit and the inner enclosure. The largest diameter is c. 80 m. The illustration shows an axial view of the complex looking west (courtesy of Aidan O' Connell, Archer Heritage Planning)

**Table 26.1** Axis azimuth from linear regression analysis

| Architectural element | Line slope obtained by regression analysis | α ° | C° | A° | Correlation coefficient $R^2$ |
|---|---|---|---|---|---|
| North side of avenue | y = 0.1310 x | 82.6 | 1.14 | 83.7 | 0.99 |
| South side of avenue | y = 0.1273 x | 82.8 | 1.14 | 83.9 | 0.98 |
| Mean | - | 82.7 | 1.14 | 83.8 | 0.99 |

The geodetic coordinates of the site are $\phi = +53°.596$ and $\lambda = -6°.589$. The longitude ($\lambda$) of the central meridian of Ireland is $-8°$. Here, the observer is located east of the central meridian and C is therefore added to the grid bearing (if west of the central meridian, C is subtracted from the grid bearing. This follows the rule that on a map projection, meridians project concave toward the central meridian and relative to the north grid line. At the central meridian, grid north and true north are parallel and C is thus zero)

where the direction of each line (m) is the tangent of the angle that the line makes with the positive direction of the x-axis. Because these data points represent plan coordinates (easting or x, northing or y), then $90° - \tan^{-1} m$ yields the grid bearing (α°) of each avenue side. The respective azimuths (A°) of the lines (avenue sides) are then obtained from

$$A = \alpha + C \tag{26.2}$$

where

$$C \approx \Delta\lambda \times \sin\phi \qquad (26.3)$$

and C = meridian convergence (the angular difference between true north and the north grid line) at the location of the site on the Transverse Mercator map projection. All units are in degrees and in the above, $\Delta\lambda$ is the difference in longitude between the site and the central meridian of the projection, and $\phi$ is the latitude of the site. Table 26.1 summarizes the method of analysis and includes the correlation coefficients (goodness-of-fit to a straight line) obtained from the site data.

The azimuth of the avenue, the altitude of the indicated horizon, and the latitude of the site were subsequently used to compute the astronomical declination indicated by the entrance avenue to the enclosure.

## Astronomical Azimuth Techniques and Instrumentation

The azimuth of any structure, or a baseline, can be obtained from the following:

- Astronomical observations (with respect to the vertical)
- Gyro station observations (with respect to the vertical)
- Geodetic observations of position (with respect to the normal to the local ellipsoid – the mathematical surface that best-fits the geoid/mean sea-level surface)
- Magnetic bearing observations

As previously described, other (indirect) methods of azimuth determination are possible, such as where a plane grid bearing is calculated from measured plane grid coordinates and then corrected for meridian convergence. In addition, azimuth can be computed using geodetic coordinates (of two points) procured from Google Earth imagery.

## Astronomical Preliminaries

Field astronomy can present significant challenges for new users in terms of the theory (see ▶ Chap. 30, "Basic Concepts of Positional Astronomy"), method of data acquisition (time and angle measurements), and processing. Here, the writer will describe a comparatively simple method which obviates the need to solve spherical equations. It is essential to use an astronomical ephemeris (a tabulation of the precise positions of celestial objects in an orderly sequence for a specified date range). One such ephemeris, and as used in the examples that follow, is MICA (Multiyear Interactive Computer Almanac).

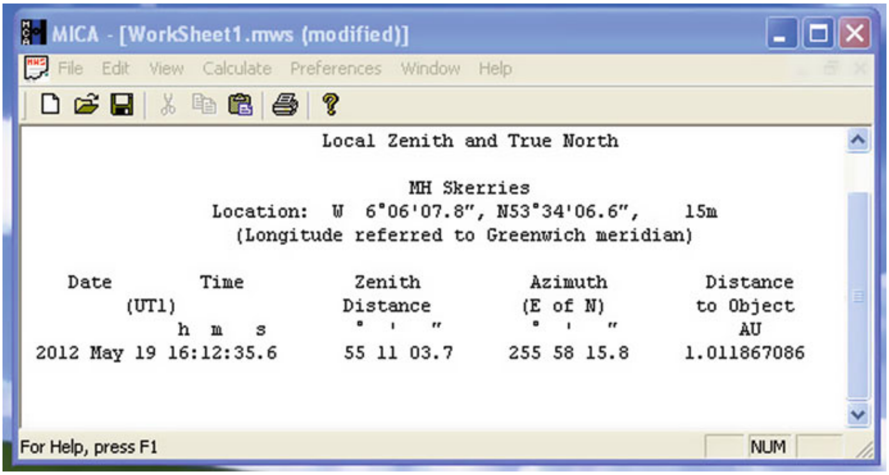


**Fig. 26.4** Screen shot from MICA of the position of the sun for place, date, and time. The position type used here is Apparent Topocentric Local Horizon. The data in Fig. 26.4 are also used in Fig. 26.7

## MICA Ephemeris

This low-cost software system is supplied on CD with an excellent instruction manual (U.S. Naval Observatory 1998–2005). It provides high-precision astronomical data in user-specified tabular form for the sun, moon, planets, and 22 bright stars. Semidiameter values of the sun and moon are also determined, as well as their zenith distances (essential if either limb of the sun or moon are observed). The current edition has a computational date range from 1800 to 2050. For any user-specified celestial object sighted with a theodolite, the geodetic location of the observation station and the time of the observation in UT1 scale (see Fig. 26.7) are first entered. The software then returns the relevant azimuth and zenith distance (90° – altitude°) as shown in Fig. 26.4. Complex calculations for azimuth are thus avoided.

Apart from the accuracy of the method, the significant advantage of this approach is in its versatility. For example, if neither the sun nor moon is above the horizon at the time of the survey, or are obscured by cloud cover, then any prominent star or planet that may be visible in the sky can be observed as an alternative. The writer has successfully used both limbs of the moon and the very bright planets and stars for azimuth, especially when these become visible in the daytime or evening sky.

For azimuth determination, correct identification of the celestial object sighted in the field is crucial. Apart from the sun and moon whose identities are certain, this is not necessarily the case with stars and planets. Mistaken identity can easily occur and with disastrous results. Practitioners should therefore exercise maximum care when sighting stars and planets and, ideally, use at least two different celestial objects for error detection purposes. For sky object identification and session

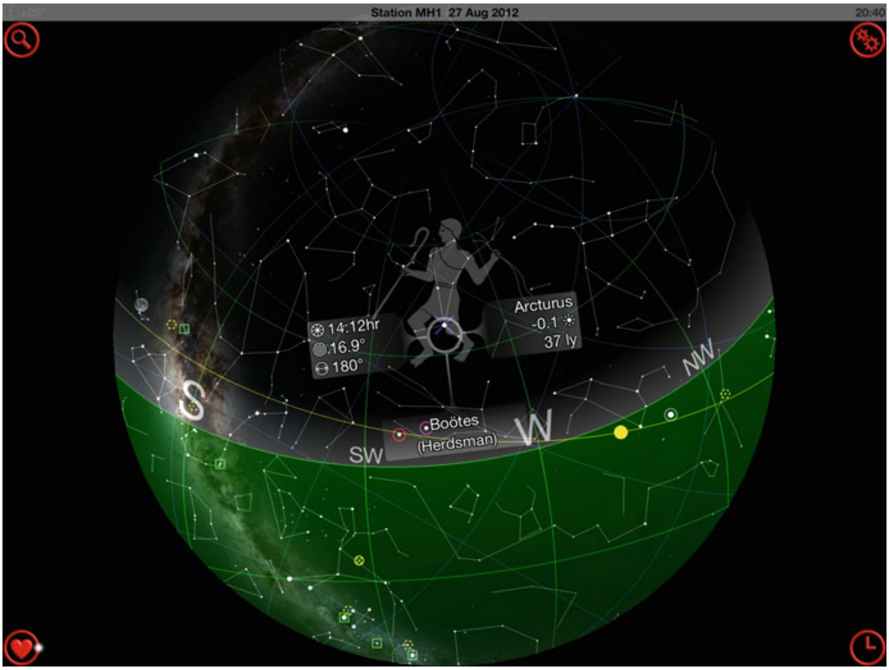


**Fig. 26.5** Field identification of stars and planets with the iPad and "Go Sky Watch" application. The device was aimed at the sky and used to confirm the identity of a suitable bright star (Arcturus) for baseline azimuth determination by the hour angle method

planning, the writer has used touch screen astronomy applications (Apps) that are compatible with, for example, the Apple iPad and iPhone. Either "Star Walk" (http://vitotechnology.com/star-walk.html), or "Go Sky Watch Planetarium" (www.gosoftworks.com/), which is freeware (Fig. 26.5), is excellent for this purpose.

Whichever tablet device is used as an aid for field astronomy, a 3 G or 4 G phone SIM card must be installed to obtain geo-referenced sky scenes in real time.

## Instrumentation for Field Astronomy

Archaeological sites of interest are invariably remote or located off-road. Where access is difficult, the overall weight of equipment that can be carried to the site becomes a crucial issue. As a general rule, minimal is best. A complete survey will typically record site description, location, orientation, horizon profile, horizon range, and intervisibility with other sites. The equipment inventory will be comprised of a field book, map(s), related literature, theodolite/total station, tripod(s), ranging pole(s), sun filter, stopwatch, measuring tape, torch, camera, and an iPad/iPhone or equivalent (optional). A GNSS (Global Navigation Satellite System)


**Fig. 26.6** (continued)

device is also essential for position finding/determination and as a time signal source in UTC (Coordinated Universal Time). Some of these devices are illustrated in Fig. 26.6.

## Astronomical Azimuth Techniques

Observing procedures for azimuth determination vary according to the application of the data. For geodetic purposes, azimuth for orientation may require rigorous observing procedures and choice of instrumentation (Bomford 1980; Ghilani 1996). For most archaeoastronomical applications, a final accuracy of several arc minutes is usually satisfactory, and this allows for a relaxation in rigor. Nonetheless, it is prudent to observe data to a higher level of accuracy than what is actually required.

In Fig. 26.7, the writer observed timed transits (hour angle method) of the left/trailing limb of the sun made with the stationary vertical stadia line of the theodolite in order to determine the azimuth of the reference object (RO). The stopwatch was initialized to UTC using the time display on a Garmin GPS60 GNSS receiver. The recorded split times of six horizontal transits of the sun's limb were then added to the initialization time of the stopwatch in UT1 scale (the astronomical time scale used by MICA to determine azimuth and other astronomical parameters). The difference (correction) between UTC and UT1 is DUT1 (see note in Fig. 26.7).

The full set of observations included three successive observations for time and direction with the theodolite in the face left (FL) position, followed by three similar observations with the theodolite in the face right (FR) position. The set commenced with a FL reading of the direction of the RO and ended with a similar reading on FR. This technique is quick, minimizes movement and handling of the theodolite and filter, and provides adequate redundancy for error checking purposes.

To demonstrate the versatility and simplicity of field astronomy for azimuth using MICA, celestial objects other than the sun's limb were additionally observed at the test baseline and at different dates. The center and left limb of the sun, various stars and planets, and the moon's limbs were each used. The resulting azimuths, including those obtained by nonastronomical methods are shown in Table 26.2 (the nonastronomical methods are discussed in sections "Gyro Station Techniques" and "Geodetic Techniques for Azimuth Determination and Location").

The accuracies shown here demonstrate the level of compatibility and consistency that can be achieved with astronomical, geodetic, and magnetic methods.

**Fig. 26.6** Instrumentation for precise azimuth observation. (**a**) A Zeiss 010B optical theodolite fitted with a Roeloff prism for precise sighting of the sun's center. (**b**) Roeloff Solar Prism objective attachment. (**c**) Homemade objective filter using Baader AstroSolar™ Safety Film. (**d**) Small torch essential for night-time illumination of the theodolite cross-hairs (when sighting a star/planet) and for reading angular directions on the horizontal circle of an analogue theodolite after sunset. (**e**) Stopwatch with good timing tactility, synchronized to UTC (see Fig. 26.7), and with a facility for recording split times

| | |
|---|---|
| Job ID | *Astronomical azimuth by hour angle of Sun* |
| Monument/Site ID | *Test baseline* |
| Baseline (from–to) | *MH Skerries—Rockabill Light (RO)* |
| Station latitude WGS84 | 53° 34′ 06″.6 N |
| Station longitude WGS84 | 06° 06′ 07″.8 W |
| Station grid easting | - |
| Station grid northing | - |
| Station height AOD (m) | 15 |
| Reference | *Field book 6/50* |
| Ephemeris | *MICA Version 2.0* |
| Observer & Instrument | FP Zeiss 010B |

**SKETCH BOX & NOTES**

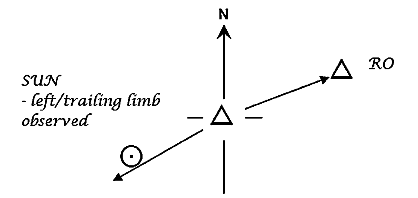


*Solar safety filter fitted to theodolite objective*

| | | | |
|---|---|---|---|
| DATE | 2012 May 19 | | |
| UTC of watch start | 16^H | 05^M | 00^S.0 |
| DUT1 (+/−) | -00 | 00 | 00.6 |
| UT1 of watch start | 16 | 04 | 59.4 |

GPS disseminates UTC time. The DUT1 correction converts UTC into UT1 - the argument used to access the precise positions (including azimuth, zenith distance) and physical parameters (including semi-diameter) of celestial bodies in MICA. UTC is kept within 0.9 sec of UT1.
DUT1 = UT1 – UTC, where DUT1 is tabulated in Bulletin A, published by IERS and is available at http://www.iers.org/IERS/EN/Publications/Bulletins/bulletins.html.

| Target | Observed direction | | | Observed split time | | | UT1 of observation | | | Azimuth of sun from ephemeris | | | Horizontal angle from RO to sun | | | Azimuth of RO | | | Sun ZD ° ′ from ephemeris | |
|---|---|---|---|---|---|---|---|---|---|---|---|---|---|---|---|---|---|---|---|---|
| | ° | ′ | ″ | H | M | S | H | M | S | | | | | | | | | | | |
| RO FL | 067 | 44 | 00 | | - | | | - | | | - | | | - | | | - | | - | |
| Sun FL | 259 | 25 | 10 | 00 | 07 | 36.2 | 16 | 12 | 35.6 | 255 | 58 | 16 | 191 | 41 | 10 | 064 | 17 | 06 | 55 | 11 |
| Sun FL | 259 | 49 | 30 | 00 | 09 | 23.1 | 16 | 14 | 22.5 | 256 | 22 | 24 | 192 | 05 | 30 | 064 | 16 | 54 | 55 | 27 |
| Sun FL | 260 | 07 | 05 | 00 | 10 | 41.1 | 16 | 15 | 40.5 | 256 | 39 | 57 | 192 | 23 | 05 | 064 | 16 | 52 | 55 | 38 |
| Sun FR | 080 | 40 | 35 | 00 | 13 | 06.8 | 16 | 18 | 06.2 | 257 | 12 | 36 | 192 | 55 | 15 | 064 | 17 | 21 | 55 | 59 |
| Sun FR | 080 | 56 | 20 | 00 | 14 | 17.5 | 16 | 19 | 16.9 | 257 | 28 | 22 | 193 | 11 | 00 | 064 | 17 | 22 | 56 | 09 |
| Sun FR | 081 | 11 | 00 | 00 | 15 | 23.7 | 16 | 20 | 23.1 | 257 | 43 | 06 | 193 | 25 | 40 | 064 | 17 | 26 | 56 | 19 |
| RO FR | 247 | 45 | 20 | | - | | | - | | | - | | | - | | | - | | - | |

If the left/right limb of the sun/moon is observed, each azimuth is corrected by the semi-diameter (SD) of the relevent body. The SD correction S = SD/Sin ZD. SD and ZD (zenith distance) are provided by MICA.
For the left/right limb, S is −/+ respectively. For archaeoastronomy, values of ZD may be rounded to the nearest arc minute with negligable error in S, and a mean correction applied.

| | | | |
|---|---|---|---|
| UTC of end signal | 16 | 28 | 00.0 |
| Split time | 00 | 23 | 00.0 |
| Watch start check | 16 | 05 | 00.0 |
| Watch error | | | 00.0 |

| | | | | |
|---|---|---|---|---|
| Mean Azimuth | 064 | 17 | 10 | |
| Semi-diameter of sun | 000 | 15 | 48 | |
| SD correction (mean) | -00 | 19 | 07 | |
| **Final Azimuth** | **063** | **58** | **03** | ±16″ |

**Fig. 26.7** (continued)

Although the Roeloff prism is no longer manufactured, it can be procured on the web. The design enables the sun's center to be directly sighted (this avoids the need for limb corrections), and for the filter to be opened and closed with ease while observing. A low-cost and safe alternative can be simply constructed from an A4 sheet of Baader AstroSolar™ Safety Film (http://www.baader-planetarium.com/sofifolie/sofi_start_e.htm). Instructions for making the filter are included with the pack. With a little practice, the sun's center can be estimated to near arc minute accuracy with such a filter and by using the cross-hair graduations of the theodolite eyepiece. Both devices are illustrated in Fig. 26.6. Overall, best results are obtained by observing celestial objects with altitudes below about 40°.

## Gyro Station Techniques

A gyro station is the combination of a theodolite and a suspended gyroscope. It is primarily designed for underground use, such as in the mining industry, although it has many other applications. All types use a suspended spinning gyro-motor/rotor which precesses in the horizontal plane due to the rotation of the earth and the effect of gravity. At any location below about latitude 75°, it will precisely define (1″–20″ depending on the model) the direction of the local meridian on the horizontal circle of the theodolite. This allows for the azimuth of any observed target or line to be easily determined (see Fig. 26.8b). A gyro station has many potential advantages, especially when used for rapid or high-accuracy orientation surveys such as inside a burial chamber, a tomb, or a building. Provided cost and availability are not an issue, its use is a viable alternative in situations where a view of the sky for

**Fig. 26.7** Observation and reduction sheet for azimuth (hour angle method). These data constitute one set of observations. Multiple sets can be observed if necessary. If a laptop computer is available, on-site reduction of the data will confirm the quality of the data and the final azimuth before leaving the site. In the example, the identity of each target sighted is shown in column 1. The observed horizontal directions of the RO (stationary) and the sun (dynamic) are shown in column 2. The recorded split times of the sun's left/trailing limb are shown in columns 3 in UTC. The UT1 of each sun-shot is shown in column 4 (UT1 of watch start + split time). The azimuth of the sun (column 5) is obtained by entering the location, date, and the UT1 of each observation in MICA. The azimuth of the RO (column 7) is obtained by subtraction of the clockwise horizontal angle between the RO and the sun (column 6) from the azimuth of the sun (column 5). Reference to the field sketch helps to avoid reduction errors. At the end of the session, a time-check of the stopwatch is undertaken as shown in Column 4. Column 8 shows the sun's zenith distance obtained in MICA (this is only required to correct limb observations). Always draw a sketch box to illustrate site relationships between the meridian, the RO, and the celestial object. Observe a compass bearing to the RO as a check for gross error. To minimize the effect of any inclination of the vertical axis of the theodolite (plate bubble error), celestial objects having an altitude higher than about 40° should not be observed. This particularly applies if using an analogue/optical instrument which does not have a dual-axis compensator. The effect of plate bubble error in such instruments is not eliminated by changing the face position (FL and FR) of the theodolite during observations. *In all cases where the sun is observed, extreme care must be taken to ensure protection of the eye*

**Table 26.2** Azimuth comparison using astronomical and nonastronomical techniques

| Method of observation | Azimuth of test baseline (L = 7.2 km) | Remarks |
|---|---|---|
| Hour angle of sun (center) | 063° 58′ 09″ | Roeloff prism was fitted to the telescope objective (see Fig. 26.6) |
| Hour angle of sun (left/trailing limb) | 063° 58′ 03″ | Baader AstroSolar™ Safety Film fitted to the telescope objective (see Fig. 26.6). Field data and computations for this example are shown in Fig. 26.7 |
| Hour angle of moon (right/leading limb) | 063° 58′ 19″ | Magnitude −12.4 |
| Hour angle of Venus | 063° 58′ 21″ | Magnitude –4.2 |
| Hour angle of Saturn | 063° 58′ 20″ | Magnitude +0.8 |
| Hour angle of Spica | 063° 58′ 04″ | Magnitude +0.16 |
| Hour angle of Arcturus | 063° 58′ 09″ | Magnitude +1.06 |
| Geodetic azimuth computed from baseline coordinates (WGS84) | 063° 58′ 00″ | Computed by Vincenty's formulae – inverse method (see section "Geodetic Techniques for Azimuth Determination and Location") |
| Plane grid bearing derived from plane grid coordinates (Irish ITM) | 063° 58′ 30″ | Plane bearing (62° 26′ 53″) computed from measured baseline grid coordinates and corrected for meridian convergence C. Using data for the observing station MH1 shown in Fig. 26.7 and equation 3, C° ≈ +01° 31′ 37″, that is, +(08°–06° 06′ 07″.8) × sin 53° 34′ 06″.7 |
| Gyro station | Not measured | See section "Gyro Station Techniques" and Fig. 26.8b |
| Magnetic compass | 064°.3 | The observed magnetic bearing (68°.3) was corrected for magnetic declination (−4°.0) |
| Theodolite App for iPad/iPhone | Variable and within ±25° of known azimuth | "Theodolite" overlays real-time information about position, altitude, bearing, range, and inclination on the device's live camera imager |

astronomical or satellite measurement is not possible. Sources of further information on these instruments are given in Table 26.3.

## Geodetic Techniques for Azimuth Determination and Location

GNSS receivers are now routinely used for a wide variety of positioning, mapping, and navigation tasks. They also disseminate time in UTC scale. Each of these properties makes them indispensible tools for archaeoastronomy. Applications include measuring the locations of sites/points of interest and baseline stations in three dimensions; deriving azimuths as an alternative to astronomical, gyro station,

**Table 26.3** Gyro station manufacturers

| Model | Further information |
|---|---|
| Gyromat | DMT http://www.gyromat.de/gyromat-3000.html |
| Gyro X | Topcon Corporation http://www.topcon.co.jp/en/positioning/sokkia/products/product/ts/gyrox.html |
| GYROMAX™ | GeoMessTechnik Heger http://www.gmt-heger.com/index.php?id=7&lang=en |

or magnetic methods; and navigating to predetermined locations in wilderness areas. Primarily, there are two types in common use, that is, high-cost survey grade receivers capable of delivering sub-centimeter levels of relative positional accuracy (Fig. 26.8a) and low-cost autonomous code-only receivers (Fig. 26.8c). The latter can deliver an instantaneous positional accuracy in plan to better than 10 m in an open sky environment. With position averaging over an extended period of time (*c*. 5 min), and with good satellite visibility (*c*. 10 satellites), the code-only type instrument can achieve an improved horizontal accuracy of up to 1–2 m. This capability makes both of these devices especially useful for azimuth determination.

With a GNSS receiver, geodetic coordinates (latitude and longitude) are determined on a mathematical model/datum, such as the WGS84 ellipsoid, of the global geoid. The direction of the shortest line between any two points on this surface (the geodesic) defines the geodetic bearing of such a line. Globally, the difference between a geodetic bearing and azimuth is extremely small (up to a few arc seconds). This permits a geodetic bearing that is calculated from a pair of coordinates to be equated for most applications (including archaeoastronomy) to azimuth as obtained by astronomical methods or with a gyro station. On a cautionary note, the accuracy of any geodetic bearing is a function of the accuracy of the relevant baseline coordinates. In turn, this is dependent upon the system/method of GNSS surveying used, that is, with a Network Real-Time Kinematic (NRTK) or any other differential system, or with a code-only handheld receiver. NRTK methods provide precise positional correction data in real time but require the user to have licensed access to a suitable broadcast infrastructure (Martin and McGovern 2012). Further information on this, and on the providers of these systems throughout Europe, is given in Table 26.4.

Azimuth and distance are now easily and precisely computed from measured/given GNSS coordinates (expressed in degree format) with the aid of online calculators. The majority of these use Vincenty's formulae (inverse method) which is a high-precision tool (Vincenty 1975). The accuracy of the derived azimuth is a function of the longitudinal and lateral position errors in the baseline coordinates and the distance between the terminal stations. Longitudinal errors (in the direction of the baseline) have no effect on azimuth accuracy. Lateral errors (at right angles to the baseline) will have maximum effect on azimuth accuracy, and this is modeled in Fig. 26.9 using three levels of assumed error. It is shown, for example, that for a lateral error of 0″.1 in the coordinates (one tenth of an arc second), the resulting error in azimuth will likely not exceed about 6 min of arc for a baseline length of about 1 km. At a range of 2 km, this reduces to about 3 min

**Table 26.4** Providers of GNSS Network RTK systems in Europe

| System | Further information |
|---|---|
| Leica Geosystems | http://smartnet.leica-geosystems.co.uk/SpiderWeb/SmartNet/smartnet.html |
| Topcon Corporation | http://www.topnetplus.eu/ |
| Trimble | http://www.trimble.com/positioning-services/vrs-now.aspx |

**Table 26.5** Comparison between azimuths derived from NRTK and Garmin GPS60 geodetic coordinates computed by Vincenty's formulae (inverse method)

| Line | Length | Azimuth (NRTK method) | Azimuth (Garmin GPS60) | Difference or error |
|---|---|---|---|---|
| 1 | 96.407 m | 304° 53′ 57″ | 304° 24′ 45″ | 00° 29′ 12″ |
| 2 | 307.531 m | 304° 47′ 40″ | 304° 21′ 28″ | 00° 26′ 12″ |
| 3 | 604.184 m | 305° 10′ 52″ | 305° 44′ 24″ | 00° 33′ 32″ |
| 4 | 1152.431 m | 305° 01′ 48″ | 305° 00′ 06″ | 00° 01′ 42″ |
| 5 | 1953.989 m | 305° 00′ 05″ | 304° 59′ 45″ | 00° 00′ 20″ |

**Table 26.6** Azimuth from Vincenty's formulae (inverse method)

| Baseline | NRTK geodetic coordinates | Garmin GPS60 geodetic coordinates |
|---|---|---|
| $\varphi^A$ | +53° 21′ 08.41339″ | 53° 21′ 08″.4 |
| $\lambda^A$ | −06° 18′ 26″.84097 | −06° 18′ 26″.7 |
| $\varphi^B$ | +53° 21′ 44″.65938 | +53° 21′ 44″.7 |
| $\lambda^B$ | −06° 19′ 53″.39326 | −06° 19′ 53″.4 |
| Azimuth (A–B) | 305° 00′ 05″ | 304° 59′ 45″ |

**Table 26.7** Online calculators and freeware for azimuth calculation from geodetic coordinates

| Author | Further information |
|---|---|
| Australian Government Geoscience Australia | http://www.ga.gov.au/geodesy/datums/vincenty_inverse.jsp |
| Wolfpack 6.1.1 by Charles D. Ghilani | http://www.personal.psu.edu/cdg3/free.htm |
| Grid InQuest v.6.6.0.1313 by Quest Geo Solutions Ltd **(for use in the UK and Ireland)** | http://grid-inquest.software.informer.com/ |

of arc. It should be appreciated that 1 arc sec at the equator is the equivalent of c. 30 m on the ground. Thus, for sub-centimeter levels of accuracy, an NRTK receiver will display geodetic coordinates to ±00″.00001 which is consistent with millimeter precision (see Table 26.6).

For verification of the modeling shown in Fig. 26.8, data was recorded at five suitably spaced stations on test baselines using a Trimble 5800 series antenna with a TSC3 logger operating in NRTK mode and a Garmin GPS60 device.

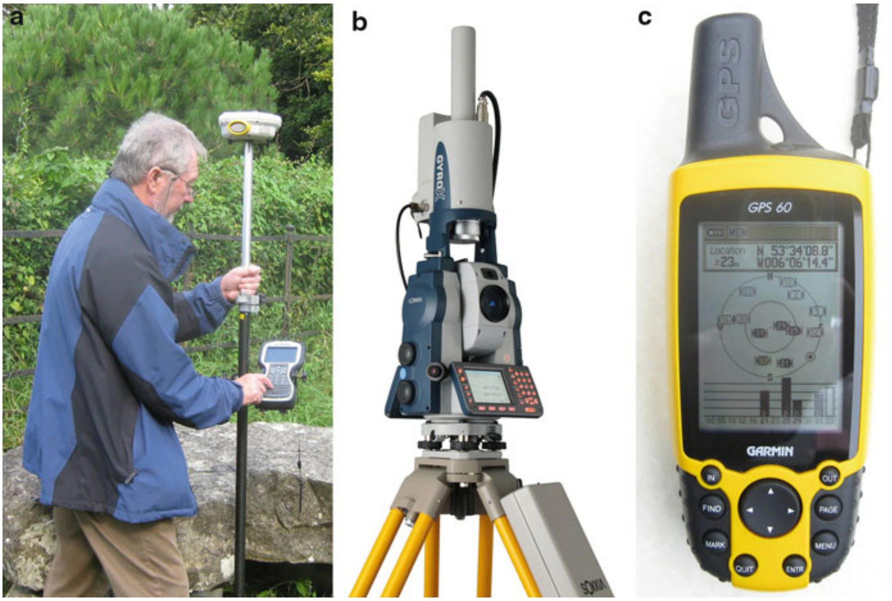


**Fig. 26.8** Geodetic instrumentation for positioning and azimuth. (**a**) A Trimble 5800 series antenna and the TSC3 logger for measuring location, site plans, or baseline/axial azimuths. (**b**) Topcon Gyro Station X for azimuth measurement (courtesy of Topcon Corporation). (**c**) Garmin GPS60 for location and baseline azimuth measurement

The results of these tests are shown in Table 26.5. Because of their very high relative accuracy, the NRTK values can be effectively regarded as error free for comparative purposes.

These tests broadly confirm the modeling shown in Fig. 26.9. The calculation of azimuth from geodetic coordinates computed with data for the longest baseline (data-line 5 in Table 26.5) is given in Table 26.6 as an example.

The online calculators tested here for the calculation of azimuth are given in Table 26.7.

The use of these techniques will facilitate azimuth calculation with ease and reliability from field coordinates recorded to an appropriate level of accuracy.

## A Tomb with a View: Synthesis and Conclusion

In the north-east midlands of Ireland, the clustered Neolithic passage tomb complex at Loughcrew consists of 31 monuments distributed on three prominent hilltops (Prendergast 2011). Three kilometers to the south-east of Cairn T, which is the highest in the distribution, an additional ruined isolate of this type is located on lower ground in the townland of Thomastown. Sufficient stones of the passage have survived to allow the passage axis to be approximately defined. A preliminary

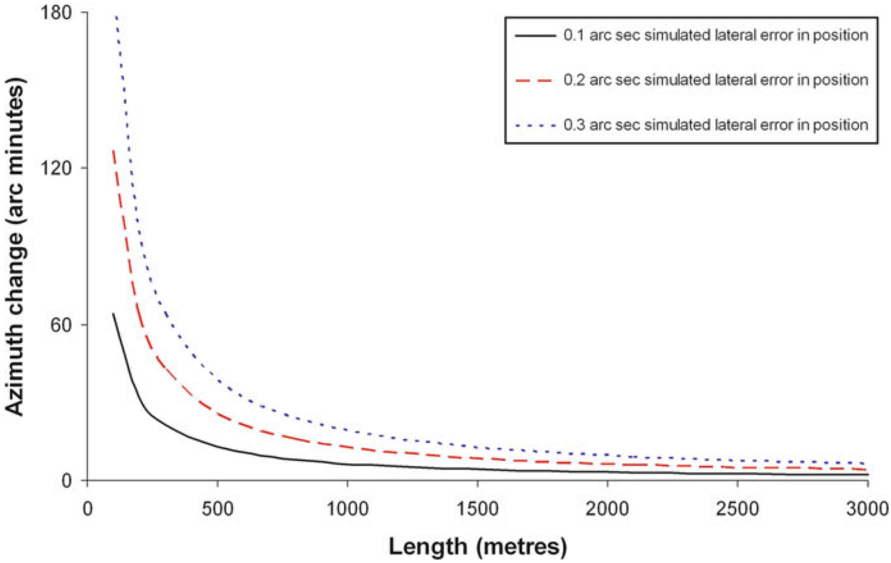


**Fig. 26.9** Accuracy modeling of azimuth from GNSS positions. The Garmin GPS60 receiver can readily achieve a positional accuracy of $\pm0''.1$ provided that data from the largest number of satellites possible is recorded and averaged (using an on-screen option) for about 5 min of time (300 measurements). Figure 26.8c shows the effect of poor visibility (signals from three satellites) and the resulting error ($\pm$23 m) in the instantaneous geodetic coordinates displayed on the screen

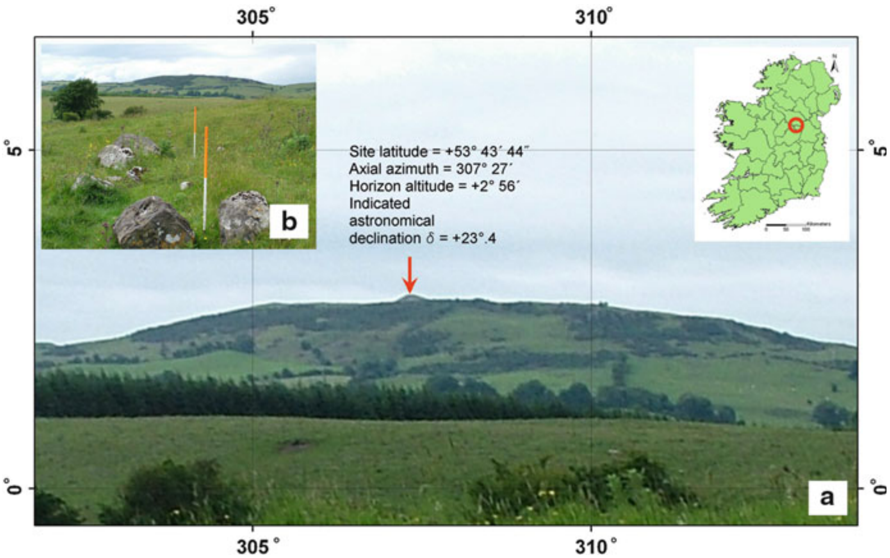


**Fig. 26.10** Survey of a passage tomb at Thomastown, Loughcrew, Ireland. (**a**) View of the hilltop horizon in the north-west and centered on Cairn T. (**b**) The ruined passage stones and estimated axial line

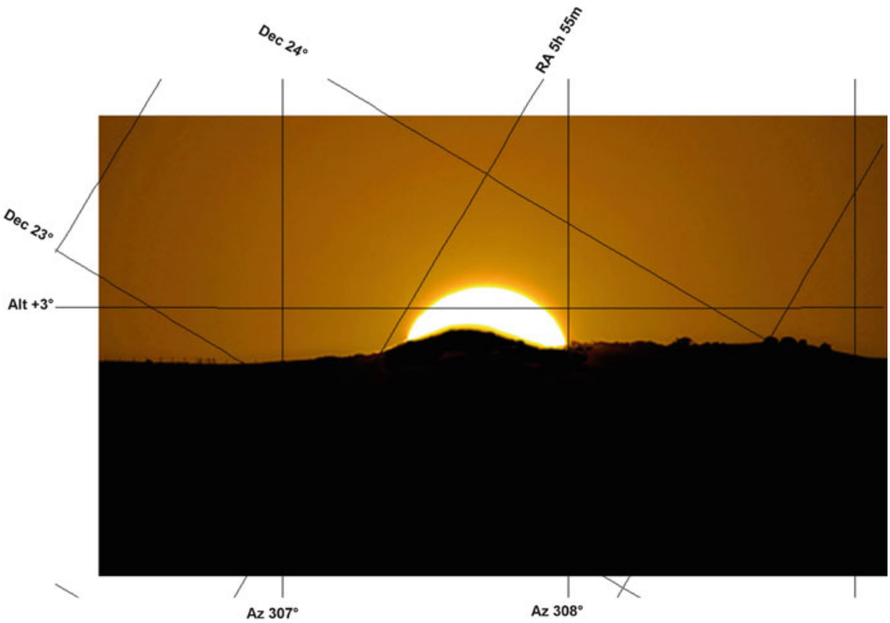


**Fig. 26.11** Summer solstice sunset behind Cairn T as viewed from the passage tomb at Thomastown. The equatorial coordinates (right ascension and declination) have been scaled to fit the local horizon coordinates. The date is 2010 June19, $20^{H}$ $32^{M}$ UTC. The writer is indebted to Ken Williams for providing site photography of the phenomenon. Freeware such as Stellarium 0.11.4 (www.winportal.com/stellarium) also allows panoramas of local landscapes/horizons to be integrated with celestial sky scenes for user-specified place and date

survey undertaken by the writer indicated the tomb (as like others in the complex) to be aligned toward the elevationally higher focal summit tomb (Cairn T). An orientation and profiling survey was subsequently undertaken to investigate this phenomenon, and any potential astronomical event of significance at this site. For this, the astronomical azimuths and altitudes of multiple natural points on the horizon were observed with a theodolite. Using these as control, the horizon image was transformed in ArcMap 10 (a component of ESRI's ArcGIS software) from arbitrary to a local topocentric horizon coordinate system (azimuth and altitude). A minimum of three observed control points are required for this type of transformation (five were used). Figure 26.10 shows the resulting gridded image.

Computation of the indicated astronomical declination of the summit tomb (see Fig. 26.10) suggested that a sunset phenomenon would also occur at the period of summer solstice. A revisit to the site observed and confirmed the expected phenomenon (Fig. 26.11).

In the Neolithic, the setting sun would have appeared tangential with the burial cairn when viewed from the tomb at Thomastown. This is due to the effect of obliquity (tilt of the earth's axis) change in the intervening 5,000 years.

Perhaps, this tomb exhibits evidence of a mingling of two culturally relevant phenomena, that is, an apparent significant astronomical alignment and an alignment that is directed at the elevationally higher and focal Cairn T at the center of the Loughcrew complex (see ▶ Chap. 24, "Nature and Analysis of Material Evidence Relevant to Archaeoastronomy"). Such a hypothesis typifies the kind of research question that confronts all archaeoastronomers, and which is addressed by this and other writers elsewhere in this volume.

## Cross-References

- ▶ Analyzing Orientations
- ▶ Basic Concepts of Positional Astronomy
- ▶ Best Practice for Evaluating the Astronomical Significance of Archaeological Sites
- ▶ Boyne Valley Tombs
- ▶ Irish Neolithic Tombs in Their Landscape
- ▶ Lunar Alignments - Identification and Analysis
- ▶ Stellar Alignments - Identification and Analysis

## References


Bomford G (1980) Geodesy. Clarendon, Oxford

Darvill TC (2002) The concise Oxford dictionary of archaeology. Oxford University Press, Oxford

De Valera R (1960) The court cairns of Ireland. Proc Roy Irish Acad 60C(2):9–140

Fraser D (1988) The orientation of visibility from chambered cairns of Eday, Orkney. In: Ruggles CLN (ed) Records in stone: papers in memory of Alexander Thom. Cambridge University Press, Cambridge, pp 9–47

Ghilani C (1996) Astronomical observation handbook. http://surveying.wb.psu.edu/sur351/CelestialCoords/ASTRO.pdf

Kelley DH, Milone EF (2005) Exploring ancient skies: an encyclopedic survey of archaeoastronomy. Springer, New York/London

Martin A, Mc Govern E (2012) An evaluation of the performance of network RTK GNSS Services in Ireland FIG Working Week 2012: knowing to manage the territory, protect the environment, evaluate the cultural heritage. Rome, Italy. http://www.fig.net/pub/fig2012/papers/ts05b/TS05B_martin_mcgovern_5582.pdf

O' Connell A (2013) Harvesting the stars: a pagan temple at Lismullin, Co. Meath. Dublin, National Roads Authority

Patat F (2011) Horizon synthesis for archaeo-astronomical purposes. Astron Notes 332(7):743–749

Prendergast F (2011) The Loughcrew hills and passage tomb complex. In: Stefanini B, Glynn GM (eds) Field Guide No. 29 - North Meath. Irish Quaternary Association, Dublin, pp 42–54

Prendergast F (2012) The Lismullin enclosure: design beyond the obvious in the Iron Age. In: Kelly B, Roycroft N et al (eds) Encounters between peoples. Archaeology and the National Roads Authority monograph series no. 9. National Roads Authority, Dublin, pp 15–30

Ruggles CLN (1999) Astronomy in prehistoric Britain and Ireland. Yale University Press, New Haven/London

Somerville BT (1923) Instances of orientation in prehistoric monuments of the British Isles. Archaeologia 73(lxxiii):193–224

Thom A (1967) Megalithic sites in Britain. Clarendon, Oxford

U.S. Naval Observatory (1998–2005) Multiyear interactive computer almanac, 1800–2050. Willmann-Bell, Richmond

Vincenty T (1975) Direct and inverse solutions of geodesics on the ellipsoid with application of nested equations. Survy Rev 176(XXXIII):88–93